Journal of Geochemical Exploration 185 (2018) 52–63

Contents lists available at ScienceDirect

Journal of Geochemical Exploration

journal homepage: www.elsevier.com/locate/gexplo

Origins of ore-forming fluid and material of the quartz–vein type Mo deposits in the East Qinling–Dabie molybdenum belt: A case study of the Qianfanling Mo deposit

Yang Gao[a,*], Jing-Wen Mao[b], Hui-Shou Ye[b], Yong-Feng Li[c]

[a] College of Earth Sciences, Jilin University, Changchun 130061, China
[b] MLR Key Laboratory of Metallogeny and Mineral Assessment, Institute of Mineral Resources, Chinese Academy of Geological Sciences, Beijing 100037, China
[c] Henan Provincial Non-ferrous Metals Geological and Mineral Resources Bureau, Zhengzhou 450016, China

ARTICLE INFO

Keywords:
Gas and liquid compositions
He-Ar isotopes
Re-Os isotopes
Qianfanling Mo deposit
East Qinling–Dabie Mo belt

ABSTRACT

The Qianfanling quartz–vein type molybdenum deposit is located in the East Qinling–Dabie Mo belt. The Mo mineralization in the deposit is mainly present as structurally controlled Mo-bearing quartz veins. Based on chromatography analysis of the Qianfanling Mo deposit, the gas compositions of fluid inclusions in quartz dominantly contain H_2O and relatively high concentrations of CO_2 (11.019 to 18.554 mol%). Cations and anions of liquid compositions of fluid inclusions are mainly Na^+ and Ca^{2+}, and SO_4^{2-} and Cl^-, respectively. The characteristics of gas and liquid compositions of fluid inclusions in quartz indicate that the Qianfanling Mo deposit formed under conditions of high oxygen fugacity. Analytical results of He-Ar isotopes of fluid inclusions in pyrite from the Qianfanling Mo deposit show that $^3He/^4He$ ratios vary from 0.02438 to 0.0796 Ra (Ra is the $^3He/^4He$ ratio of air = 1.40×10^{-6}), with F^4He values of 252,509–885,224. The calculated He_{mantle} values range from 0.18 to 0.87%, with an average of 0.39%. $^{40}Ar/^{36}Ar$ ratios are 694.4–1473.4, with the estimated $^{40}Ar^*$ (radiogenic ^{40}Ar) proportion of 79.9%. These He-Ar isotopic data indicate that most of the He in the fluid inclusions was derived from the crust, with negligible atmospheric He and only a very small input from the mantle probably. Furthermore, the Ar in the ore-forming fluid was mainly derived from the crustal source, with minor atmospheric Ar involved. 17 Re–Os model ages of 15 molybdenite samples from the 4 quartz-vein type Mo deposits (Qianfanling, Daxigou, Maogou, and Zhifang) range from 215.0 to 248.2 Ma, with a mean value of 235.6 Ma, which is close to the age of peak collision between the North China and Yangtze Cratons. The Re contents in molybdenite from the 4 deposits range from 0.19 to 39.16 ppm, with an average of 17.41 ppm, indicating a crust-dominated source. Re contents in molybdenite from Mesozoic Mo deposits in different ages and types in the East Qinling–Dabie Mo belt show different characteristics of ore sources. Combined with gas and liquid compositions and He-Ar isotopic characteristics of fluid inclusions, as well as Re contents in molybdenite of this paper and previous studies, we suggest that the ore-forming fluid and material of the Qianfanling Mo deposit were mainly derived from crustal magmatic source. This magmatic source could have formed by partial melting of deep crustal rocks under a certain condition during the collision between the North China and Yangtze Cratons.

1. Introduction

The East Qinling–Dabie orogenic belt, located between the North China and Yangtze Cratons (Zhang et al., 1996; G.W. Zhang et al., 2001), is an important metallogenic belt for Au, Ag, Pb, Zn, W, and Sb, and especially the most important Mo ore province in China (Luo et al., 1991; Xie et al., 2001; Z.W. Zhang et al., 2001; Mao et al., 2005, 2009; Li et al., 2005; Liu et al., 2007; Li et al., 2008; Chen et al., 2017). The extensive Mesozoic tectono-magmatic-metallogenic events occurred in the East Qinling–Dabie orogenic belt, the most remarkable result of which is the formation of one of the most important Mo ore districts in the world, named the East Qinling–Dabie Mo belt (Mao et al., 2008; J.W. Mao et al., 2011; Fig. 1), with measured reserves of > 8 Mt of Mo metal (J.W. Mao et al., 2011). Three episodes of the Mesozoic Mo mineralization in the East Qinling–Dabie Mo belt have been recognized on the basis of the deposit characteristics and tectonic settings (Mao et al., 2008; J.W. Mao et al., 2011), i.e., Triassic, Late Jurassic to Early Cretaceous, and Early to middle Cretaceous.

* Corresponding author at: College of Earth Sciences, Jilin University, No. 2199 Jianshe Street, Changchun 130061, China.
E-mail address: yanggao@jlu.edu.cn (Y. Gao).

https://doi.org/10.1016/j.gexplo.2017.11.005
Received 19 May 2017; Received in revised form 28 August 2017; Accepted 9 November 2017
Available online 11 November 2017

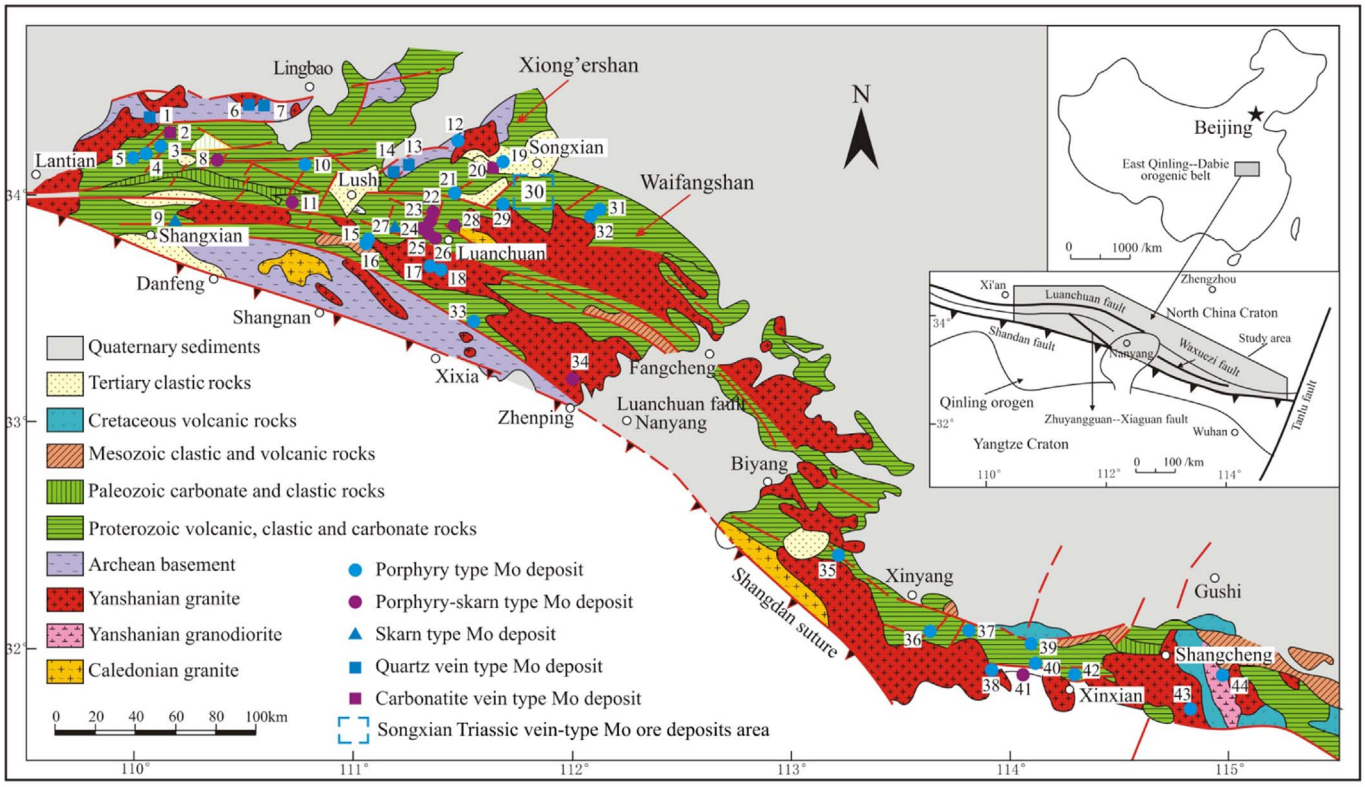

1) Xigou, 2) Huanglongpu, 3) Shijiawan, 4) Jinduicheng, 5) Balipo, 6) Majiawa, 7) Dahu, 8) Mulonggou, 9) Nantai, 10) Yinjiagou, 11) Yechangping, 12) Shapoling, 13) Longmendian, 14) Zhaiwa, 15) Saozhoupo, 16) Donggoukou, 17) Laojieling, 18) Nangou, 19) Leimengou, 20) Huangshui' an, 21) Shiyaogou, 22) Majuan, 23) Nannihu-Sandaozhuang, 24) Shangfanggou, 25) Zhuyuangou, 26) Dawanggou, 27) Huoshenmiao, 28) Luocun, 29) Yuchiling, 30) Songxian Triassic vein-type Mo ore deposits area including Cangfangyuan, Shenmagou, Fantaigou, Xiangchungou, Zhaigou, Qianfanling, Dawanggou, Zhifang, Tulingcun, Maogou, Daxigou and Daqiaogou Mo ore deposits, 31) Donggou, 32) Zhuyuangou (Ruyang), 33) Banchang, 34) Qiushuwan, 35) Tianmushan, 36) Xiaofan, 37) Mushan, 38) Doupo, 39) Qian'echong, 40) Bao'anzhai, 41) Dayinjian, 42) Yaochong, 43) Tangjiaping, 44) Shapinggou

Fig. 1. Simplified geological map, showing the distribution of different types of Mo deposits in the East Qinling-Dabie orogenic belt (after J.W. Mao et al., 2011).

The formation of the quartz–vein type Mo deposits, which occurred in the central part of Songxian County, Henan Province, represent the earliest Mo metallogenetic event of the Mesozoic Mo mineralization in the East Qinling–Dabie Mo belt (Y. Gao et al., 2010; Deng et al., 2017). The forming ages of these quartz–vein type Mo deposits are close to the date of collision between the North China and Yangtze Cratons (242–219 Ma; Ames et al., 1993; Chen et al., 1995; Eide et al., 1994; Liou et al., 1996; Hacker et al., 1998). These structurally controlled, apparently intrusion-unrelated quartz–vein type Mo deposits are distinguished from other Mo deposits in the same orogenic belt and even in other Mo ore districts worldwide.

On the basis of analytical results of fluid inclusions and stable isotopes (H-O-C-S) of the Qianfanling Mo deposit, a representative quartz–vein type Mo deposit, Gao et al. (2013) proposed that the sulfur and ore-forming fluid of the deposit were derived from a deep-seated igneous source, and fluid immiscibility is the main mechanism for crystallization of ore minerals. However, the ore-forming fluids and materials sources of the Qianfanling Mo deposit and other quartz–vein type Mo deposits are still unclear, e.g., whether there were any mantle-derived fluids and metals have been involved in the mineralization process.

In this paper, we present gas and liquid compositions and He-Ar isotopic data of fluid inclusions hosted in quartz and pyrite from the Qianfanling Mo deposit, in order to constrain the nature and source of ore-forming fluid of the deposit. We also discuss ore material sources of the quartz–vein type Mo deposits and other Mesozoic Mo deposits in different ages and types in the East Qinling–Dabie Mo belt, based on the Re contents in molybdenites from these Mo deposits. In addition, implications for tectonic setting and ore genesis of the quartz–vein type Mo deposits will also be briefly discussed.

2. Regional geology

The East Qinling–Dabie orogenic belt (Fig. 1) is part of the 2000 km long Qinling–Dabie orogen, which was formed as a result of collision events between the North China and Yangtze Cratons during the Early Silurian and Late Triassic (Ames et al., 1993; Hacker et al., 1996; Kröner et al., 1993). The Early Silurian Shangdan Suture divides the orogenic belt into the North and South Qinling zones, with South Qinling and the Yangtze Craton to the south being separated by the Late Triassic Mianlue Suture (G.W. Zhang et al., 2001) and the Luanchuan Fault, marking the boundary between North Qinling and the North China Craton.

The southern margin of the North China Craton is bounded by two NWW-trending faults: the Sanmenxia–Lushan Fault to the north and the Luanchuan Fault to the south, which separates the craton from the North Qinling orogenic belt. The basement in this region is composed of Late Archean (ca. 2.6–2.9 Ga) gneiss, granulite, and migmatite of the Taihua Group (G.W. Zhang et al., 2001), which is disconformably overlain by the Mesoproterozoic (ca. 1.78 Ga) Xiong'er Group. The dominant basaltic andesites and andesites of the Xiong'er Group, along with minor dacites and dacitic rhyolites, outcrop over an area of 60,000 km^2 (Guo et al., 2006) and are thought to be either arc-related (He et al., 2008) or part of a large igneous province (Peng et al., 2008; Pirajno et al., 2009). The volcanic rocks of the Xiong'er Group are overlain by littoral clastic rocks, volcanic rocks and carbonate rocks of Proterozoic age; as in other parts of the North China Craton, Upper Ordovician to Lower Carboniferous strata are absent. Discordantly overlying these sediments are Middle–Upper Carboniferous terrigenous clastic rocks intercalated with marine carbonates and coals, which are in turn overlain by Permian coal-bearing terrigenous clastic rocks. Triassic alluvial and fluvial facies clastic rocks, Jurassic continental

sediments, and Cretaceous lacustrine volcano-sedimentary rocks are also locally present, with andesitic porphyries intruding Cretaceous basin sediments at ca. 131.8–117 Ma, as dated by SHRIMP zircon U–Pb analysis (Wang et al., 2002; Xie et al., 2007).

The granitic magmatism in the East Qinling–Dabie orogenic belt occurred from the Late Archean (2.9–2.5 Ga) to the Mesozoic (ca. 80 Ma) (Lu, 1999; Sun et al., 2003; Wang et al., 2003, 2009; Zhang et al., 2008; Wang et al., 2011a, 2011b). Six pulses of granitoid magmatism in the East Qinling–Dabie orogenic belt have been recognized (Lu, 1999 and references therein): Late Archaean (2.9–2.5 Ga) tonalite–trondhijemite–granodiorite, Early Proterozoic (2.0–1.6 Ga) A–type granites, Late Proterozoic (1.1–0.8 Ga) and Early Paleozoic (600–420 Ma) subduction–, collision– and post–collision related granites, and Mesozoic granite emplacement. The Mesozoic, especially during the Jurassic to Cretaceous, is the most significant period for granitoid emplacement in the East Qinling–Dabie belt. The late Mesozoic Mo mineralization in the East Qinling–Dabie Mo belt is temporally–spatially related to the contemporaneous intermediate–felsic magmatism in the region (e.g., Mao et al., 2010; Li et al., 2013). The ore-associated porphyries of the majority of porphyry (-skarn) type Mo deposits are the products of the magmatism. In addition to the Mo deposits, the East Qinling–Dabie orogenic belt also hosts a number of other mineral deposits, most importantly Au, Ag, Pb, and Zn deposits (Mao et al., 2002, 2009; Li et al., 2008).

The quartz-vein type Mo deposits were discovered in the contact zone between the Xiong'ershan and Waifangshan districts (Figs. 1, 2a), the southern margin of the North China Craton. A total of 12 Mo deposits containing > 30 individual molybdenite–quartz veins have been discovered in central Songxian County, Henan Province, forming the Songxian quartz-vein type Mo ore concentration area. The outcrop in the area consists of Xiong'er Group volcanic rocks and Palaeogene and Quaternary sediments, with NE and NW trending regional faults. Proterozoic granodiorites and Mesozoic syenites (Mogou pluton, 208.5 ± 6.2 Ma, Ren et al., 1996) and granites (Heyu pluton (148.2–135.3 Ma, X.Y. Gao et al., 2010), Taishanmiao pluton (115 ± 2 Ma, Ye et al., 2008), and several other small plutons) also outcrop in the study area (Fig. 2a). The Mo mineralization in these quartz-vein type Mo deposits could be divided into quartz-vein type and disseminated type. Most of the Mo mineralization is present as molybdenite-quartz veins (Fig. 3). All of the Mo-bearing quartz veins are hosted by Mesoproterozoic andesitic–dacitic–rhyolitic rocks and tuffs of the Xiong'er Group. The veins are generally 300–1600 m in length, 2–7 m in thickness, and NE dipping. Wall rock alteration is characterized by development oriented parallel to both sides of quartz veins, mainly including Silicification, K-feldspar alteration, propylitic alteration, and Sericitization.

3. Geological characteristics of the Qianfanling Mo deposit

In the Qianfanling Mo deposit, Xiong'er Group volcanic rocks, Quaternary sediments, and a post-ore granite dike crop out (Fig. 2b). In addition, two large faults cross-cut the granite dike and are not spatially related to the main Mo-bearing veins, indicating that these faults are not related to the formation of the deposit. Many small faults and joints are present within the deposit and control the distribution of the Mo-bearing quartz veins. Three main Mo-bearing veins (numbered as P1, P2 and P3) are exposed in the Qianfanling Mo deposit (Fig. 2b), whereas other quartz veins are thinner than these three veins and are exposed underground as veinlet or stockwork networks. Of the three main Mo-bearing veins, the P2 vein is the longest, at around 1000 m in length, and is 2–4 m in thickness (Fig. 2c).

The Mo ores in the deposit could be divided into two types: quartz-vein type and disseminated type. The quartz-vein type ores (Fig. 3a, b) occur as molybdenite-quartz veins; the disseminated type ores are characterized by molybdenite and other sulfides developed in the altered wall rocks. In quartz-vein type ores, the main ore minerals are molybdenite and pyrite, with minor galena. Gangue minerals are dominantly quartz and barite, with minor calcite. In the altered wall rocks, the main ore minerals are molybdenite and pyrite. The ore minerals show the textures including: (1) euhedral, subhedral, and anhedral granular textures; (2) replacement and remnant replacement textures; (3) deformed and cataclastic textures.

Wall rock alteration in the Qianfanling Mo deposit is developed along and adjacent to mineralized fracture zones. Silicification is the dominant alteration in the Qianfanling Mo deposit and is represented by quartz, which replaced plagioclase phenocrysts and matrix of the wall rocks. K-feldspar alteration is represented by the mineral assemblage of K-feldspar and quartz. Alone and close to quartz veins, K-feldspar occurs as irregular replacement of phenocrysts and matrix of the wall rocks. Pyritization led to the formation of disseminated pyrite crystals (1–2 mm), which are generally associated with K-feldspar alteration. Carbonate is characterized by the formation of calcite. Sericitization is always associated by epidotization and chloritization, characterized by the formation of disseminated sericite, epidote, and chlorite.

On the basis of cross-cutting relationships among ore veins, mineral assemblages, paragenetic sequence, and ore fabrics, the mineralization can be divided into three stages: (1) Stage I is characterized by the development of pyrite–barite–quartz veins and a Mo-free pyrite, barite, and quartz mineral assemblage with minor calcite and K-feldspar; (2) Stage II is characterized by formation of Mo-bearing quartz veins, with molybdenite and pyrite forming the main ore minerals; (3) Stage III is characterized by the development of quartz–calcite or calcite veins, and represents a late stage of the hydrothermal activity.

4. Sampling and analytical methods

4.1. Chromatography analysis

After the ores were crushed, six quartz samples (QFL-B-12 and QFL100720-11 from stage I; others from stage II) from the Qianfanling Mo deposit were handpicked under a binocular microscope (0.2–0.4 mm in size, purity > 99%). The pure quartz were then heated to open the fluid inclusions in the minerals and the gas and liquid compositions were determined by chromatography. The chromatography analysis were carried out in the MLR (Ministry of Land and Resources) Key Laboratory of Metallogeny and Mineral Assessment, Institute of Mineral Resources, Chinese Academy of Geological Sciences, Beijing. The gas and liquid compositions were measured using a GC2010 two-dimensional gas chromatograph and an HICSP super ion chromatograph made in Shimadzu Corporation of Japan, respectively. The blast furnace was made in SGE Corporation of Australia. The decrepitation temperature ranged from 100 °C to 500 °C. The detection limits were 10^{-6} for cations and 10^{-9} for anions, respectively. Detailed measurement procedures are described by Yang et al. (2007).

4.2. He-Ar isotope analysis

Five ore samples of the Mo-forming stage from the Qianfanling Mo deposit were collected from underground mine workings (P2 Mo-bearing quartz vein) for He and Ar isotopic analysis. After the samples were crushed, pyrite chips (0.25–1 mm in size) were hand-picked under a binocular microscope (purity > 99%). He and Ar isotopic analysis was performed at the Lanzhou Center of Oil and Gas Resources, Institute of Geology and Geophysics, Chinese Academy of Sciences, using a Micromass MM5400 gases mass spectrometer. Analytical conditions were It_4 = 800 μA, It_{40} = 200 μA, and at a high pressure of 9.000 kV. All weighed samples of pyrite for analysis were packed into aluminum foil and shifted to the crucible for gas extraction under high vacuum conditions. When a pressure lower than 1×10^{-5} Pa was attained, the samples were heated at 130 °C for at least 10 h to eliminate secondary fluid inclusions and trace gases occurring in cleavages or

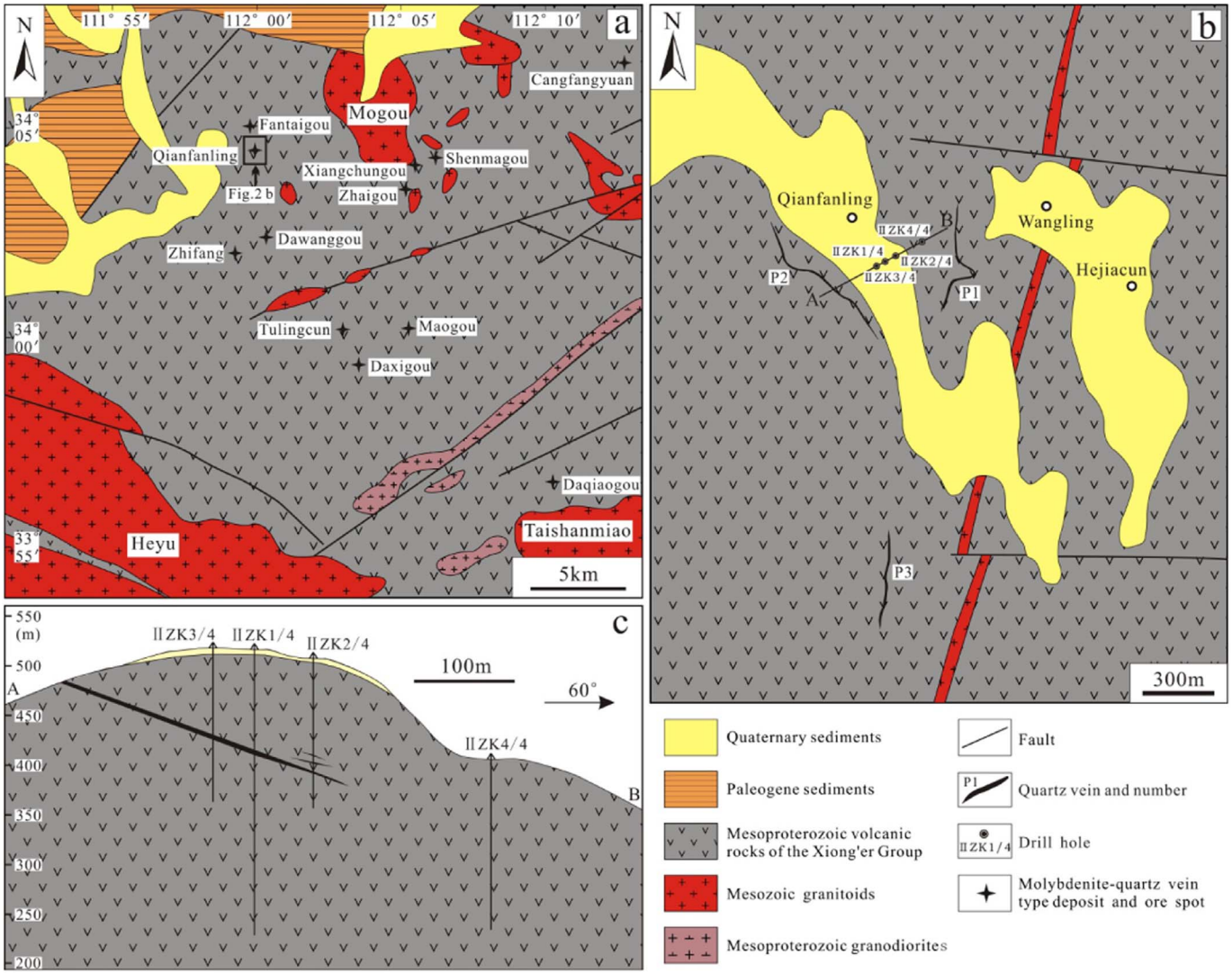

Fig. 2. (a) Plan view of the Triassic quartz vein Mo deposits in Songxian County, Henan Province (after Y. Gao et al., 2010). (b) Simplified geological map of the Qianfanling Mo deposit (modified from Luoyang Zhongmai Mining Company, 2008). (c) Geological cross-section through the Qianfanling Mo deposit along exploration line 4 (modified from Luoyang Zhongmai Mining Company, 2008).

fractures in the crusts. Then, the samples were fused at high temperatures of up to 1600 °C, and the released gases were purified through activated charcoal traps at the liquid nitrogen temperature to separate He and Ar from Ne + Kr + Xe for He and Ar analysis on the mass spectrometer, respectively. The minimum heat blanks for the MM5400 mass spectrometer at 1600 °C (cm^3 STP) are: $^{4}He = 2.46 \times 10^{-10}$, $^{20}Ne = 4.08 \times 10^{-10}$, $^{40}Ar = 1.39 \times 10^{-8}$, $^{84}Kr = 3.07 \times 10^{-12}$, and $^{132}Xe = 1.26 \times 10^{-13}$ in units of mol. The standard for normalizing the analytical results is air in Lanzhou (AIRLZ2007); analytical precision for the noble gases isotopic measurements is better than 10%. Detailed sample preparation and measurement procedures are described by Ye et al. (2007).

4.3. Molybdenite Re–Os isotope analysis

Fifteen molybdenite samples of the Qianfanling, Daxigou, Maogou, and Zhifang Mo deposits were selected for Re–Os isotope analysis using an optical microscope and then fresh, non-oxidized molybdenite grains (0.2–0.5 mm in size) were magnetically separated and handpicked using a binocular microscope (purity > 99%). Re–Os isotope analysis was carried out in the Re–Os laboratory at the National Research Center of Geoanalysis, Chinese Academy of Geological Sciences, Beijing. The details of the Re–Os chemical separation procedures have been described by Du et al. (1994) and Markey et al. (1998). Carius tube digestion was used in this study, whereby samples were digested in a thick-walled borosilicate glass ampoule. In brief, molybdenite was dissolved and equilibrated with ^{185}Re and ^{190}Os spikes. Osmium was distilled as OsO_4 from an H_2SO_4–$Ce(SO_4)_2$ solution, and separation of Re from the remaining solution was achieved by solvent extraction and cation-exchange resin chromatography. Re and Os isotope ratios were determined by a TJA X-series inductively coupled plasma–mass spectrometer (ICP–MS). During the course of this study, Re blanks were < 11 pg and ^{187}Os blanks were < 0.2 pg. The uncertainty on each individual age determination was ca. 1.4%, including uncertainties on the ^{187}Re decay constant, isotope ratio measurements, and spike calibrations. A ^{187}Re decay constant of $1.666 \times 10^{-11}\ y^{-1}$ was used and has an absolute uncertainty of $\pm 0.017 \times 10^{-11}\ y^{-1}$ ($\pm$ 1.0%; Smoliar et al., 1996). The Re–Os isochron was calculated using the ISOPLOT software (Ludwig, 2003).

Fig. 3. characteristics of mineralization and alteration of the representative quartz vein-type Mo deposits in Songxian Triassic vein-type Mo deposits area.
a-b. Molybdenite-bearing quartz vein at the surface, and Molybdenite assemblage in the quartz vein (Qianfanling); c. Mo-bearing quartz vein and Mo-barren quartz vein (Daxigou); d. drill core shows Mo-bearing quartz vein, and K-feldspar and propylitic alteration (Daxigou); e. molybdenite-bearing quartz vein (Maogou); f. strong K-feldspar alteration caused by molybdenite-bearing quartz stockwork; g. outcrop of Molybdenite-bearing quartz vein (Zhifang); h. massive molybdenite-bearing quartz-vein type ore (Zhifang). Abbreviations: Mo-molybdenite.

5. Analytical results

5.1. Composition of fluid inclusions

Gas and liquid compositions of fluid inclusions in quartz samples from the Qianfanling Mo deposit are shown in Tables 1 and 2. H_2O is the dominant component in gases of all of the samples, ranging from 66.663 to 82.084 mol%. It is worth noting that all of the samples have relatively high concentrations of CO_2 in fluid inclusions, varying from 11.019 to 18.554 mol%. Additionally, the fluid inclusions in all of the samples contain lesser amounts of N_2, O_2, and CO, and trace amounts of CH_4, C_2H_2 + C_2H_4, and C_2H_6.

Cations of liquid composition of the fluid inclusions mostly consist of Na^+ and Ca^{2+}, ranging from 5.042 to 36.059 μg/g and 10.984 to 26.628 μg/g, respectively. Compared to Na^+ and Ca^{2+}, the contents of K^+ and Mg^{2+} are relatively low. Notably, the Li^+ contents of all samples are extremely low. Anions of liquid composition are mainly SO_4^{2-} and Cl^-, ranging from 10.666 to 43.489 μg/g and 3.523 to 20.386 μg/g, respectively, followed by small amounts of NO_3^-, F^-, and Br^-.

Table 1
Analytical results of gas chromatography of fluid inclusions in quartz from the Qianfanling Mo deposit.

Sample	CH_4		C_2H_2 + C_2H_4		C_2H_6		CO_2		H_2O		O_2		N_2		CO	
	μg/g	mol%	μg/g	mol%	μg/g	mol%	μg/g	mol%	μg/g	mol%	μg/g	mol%	μg/g	mol%	μg/g	mol%
QFL-B-12	1.045	0.109	0.099	0.003	–	–	289.586	11.019	882.475	82.084	16.509	0.864	80.187	4.795	18.826	1.126
QFL100720-11	0.806	0.100	0.302	0.011	0.165	0.011	410.018	18.554	637.683	70.536	16.822	1.047	87.647	6.232	49.350	3.509
QFL-3	4.918	0.546	0.145	0.005	0.027	0.002	384.328	15.505	748.794	73.843	21.724	1.205	106.788	6.770	33.521	2.125
QFL-12	0.135	0.083	0.042	0.008	–	–	68.682	15.290	127.280	69.265	8.015	2.453	36.875	12.900	–	–
QFL-44	0.146	0.061	0.018	0.002	–	–	84.360	12.714	180.951	66.663	17.148	3.554	71.810	17.007	–	–
QFL100718-7	0.258	0.086	0.053	0.005	–	–	131.239	15.972	238.993	71.097	12.611	2.110	56.105	10.730	–	–

Note: – is below the detection.

5.2. He-Ar isotopes

The results of He and Ar isotope analysis of fluid inclusions hosted in pyrite from the Qianfanling Mo deposit are listed in Table 3. The concentrations of ^{4}He and ^{40}Ar are 240–800 × 10^{-7} cm^3 STP/g and 3.84–11.12 × 10^{-7} cm^3 STP/g, respectively. The R/Ra ratios of the ore-forming fluid from the pyrite samples are 0.02438–0.0796 (R and Ra represent the ^{3}He/^{4}He ratios of the samples and air (1.40 × 10^{-6})), respectively. ^{40}Ar/^{36}Ar ratios are 694.4–1473.4.

5.3. Re-Os isotopes

Re and Os abundances and isotopic data for the 15 molybdenite samples from the four quartz-vein type Mo deposits are presented in Table 4. The Re contents in molybdenite range from 0.19 to 39.16 ppm, with an average of 17.41 ppm. The ^{187}Re and ^{187}Os concentrations vary from 0.12 to 24.61 ppm and 0.48 to 97.07 ppb, respectively. 17 Re–Os model ages of the 15 samples range from 215.0 ± 3.1 to 248.2 ± 3.5 Ma, with a mean value of 235.6 ± 1.5 Ma.

6. Discussion

6.1. He-Ar isotopes and source of the ore-forming fluid

6.1.1. Reliability of the He-Ar isotopic compositions

Previous studies have shown that the He-Ar isotopes can be used to trace the origin of fluids in ancient metallic deposits (e.g., Turner et al., 1993; Stuart et al., 1995; Hu et al., 2004). Pyrite is known to be a suitable trap for noble gases (Burnard et al., 1999). However, the extent of post-trapping modification, including in situ radiogenic production of ^{4}He and ^{40}Ar, cosmogenic ^{3}He, and He loss by diffusion (e.g., Burnard et al., 1999; Ballentine and Burnard, 2002; Hu et al., 2012) must be considered before using He-Ar isotopes to constrain the origin of ore-forming fluids.

The pyrite samples analyzed in this study were collected from Mo-forming stage ores with no sign of subsequent modification. The fluid inclusions in pyrite, therefore, were probably related to the mineralization. The measured He in fluid inclusions in pyrite from the Qianfanling Mo deposit is not the product of nuclear decay of Li due to the absence of Li-bearing minerals (Ballentine and Burnard, 2002). The hydrothermal fluids usually contain very low concentrations of U and Th (Norman and Musgrave, 1994). Moreover, after the trap of fluid inclusions, the in situ produced ^{4}He from nuclear decay of U and Th in the pyrite lattice could not diffuse into the fluid inclusions (Simmons et al., 1987; Stuart and Turner, 1992; Stuart et al., 1995). Thus, the ^{4}He that was decayed by U and Th is negligible. Cosmogenic He is not considered to be a source of ^{3}He because all samples were collected from underground mine workings (Ballentine and Burnard, 2002). Significant contributions of in situ produced ^{40}Ar from the mineral lattice to the measured ^{40}Ar/^{36}Ar ratios is thought unlikely due to the low diffusivity of Ar and low K concentrations in pyrite (York et al., 1982; Smith et al., 2001).

It has been established that pyrite with inclusions trapped He remains closed on a timescale of 100 Ma (e.g., Turner and Stuart, 1992; Baptiste and Fouquet, 1996). The mineralization age of the Qianfanling Mo deposit is 239 Ma (Y. Gao et al., 2010), therefore, the result of calculation reveals that He has diffused in the pyrite lattice over an area of 0.75 × 10^{-4} cm^2, according to a diffusion coefficient of 10^{-20} cm^2/s (Baptiste and Fouquet, 1996). He activity in fluid inclusions is several orders of magnitude lower than that of the lattice (Trull et al., 1991), so little He has been lost from the fluid within the 239 Ma since the formation of the ore deposit. In addition, the finer the minerals are crushed, the more radiogenic ^{4}He will be released from the mineral lattice (Stuart et al., 1995). However, experimental studies have shown that ^{3}He/^{4}He remains constant during the crushing process, indicating that only negligible radiogenic ^{4}He is released from the mineral lattice and/or that He diffusion through pyrite is sufficiently slow to prevent He loss during crushing (Hu et al., 2009).

Therefore, we believe that the analytical data in this study could represent the initial He and Ar isotopic compositions of the ore-forming fluid trapped in the fluid inclusions during mineralization of the Qianfanling Mo deposit.

6.1.2. He-Ar isotopic compositions and the geological implications

He and Ar isotopes trapped in hydrothermal fluids have three potential sources (Turner et al., 1993; Stuart et al., 1995; Burnard et al., 1999): (1) air-saturated water (ASW), including meteoric water and seawater, which has a typical He and Ar isotopic composition of ^{3}He/^{4}He = 1 Ra = 1.4 × 10^{-6}, ^{40}Ar/^{36}Ar = 295.5; (2) mantle-derived fluids, which contain high ^{3}He and low ^{36}Ar, with ^{3}He/^{4}He ratios generally of 6–9 Ra, and Ar is dominated by radioactive ^{40}Ar, ^{40}Ar/^{36}Ar ≥ 40,000; (3) crust-derived fluids, the characteristic values

Table 2
Analytical results of ion chromatography of fluid inclusions in quartz from the Qianfanling Mo deposit (μg/g).

Sample	Na^+	K^+	Mg^{2+}	Ca^{2+}	F^-	Cl^-	Br^-	NO_3^-	SO_4^{2-}
QFL-B-12	25.269	12.015	1.119	13.759	0.333	12.378	0.095	0.167	26.078
QFL100720-11	22.705	11.513	0.386	10.984	0.226	10.645	0.077	0.053	23.751
QFL-3	29.032	6.559	1.677	18.382	0.488	20.386	0.244	0.541	24.650
QFL-12	5.042	1.071	1.870	26.628	0.236	3.523	0.073	0.230	10.666
QFL-44	14.212	10.580	1.199	20.162	0.067	6.721	0.161	0.168	18.661
QFL100718-7	36.059	12.962	2.167	25.456	0.295	16.706	0.353	0.288	43.489

Table 3
He-Ar isotopic compositions of fluid inclusions trapped in pyrite from the Qianfanling and five Mesozoic porphyry (-skarn) Mo deposits in the East Qinling–Dabie Mo belt.

Sample	Deposit	$^4He \times 10^{-7}$ (cm^3 STP/g)	$^{40}Ar \times 10^{-7}$ (cm^3 STP/g)	R/Ra	$^{40}Ar/^{36}Ar$	$^{40}Ar^*/^4He \times 10^{-3}$	$^{40}Ar^*$ (%)	F^4He	He_{mantle} (%)	References
QFL-18	Qianfanling	495 ± 33	3.84 ± 0.27	0.02798 ± 0.00055	1052.2 ± 48.6	5.58	79.9	822,031	0.23	This study
QFL-36	Qianfanling	240 ± 16	4.00 ± 0.30	0.04175 ± 0.00016	694.4 ± 11.0	9.57		252,509	0.40	
QFL-52	Qianfanling	800 ± 54	8.07 ± 0.56	0.02438 ± 0.00030	1473.4 ± 36.7	8.06		885,224	0.18	
QFL-53	Qianfanling	544 ± 37	6.65 ± 0.47	0.02960 ± 0.00028	947.1 ± 27.5	8.41		469,558	0.25	
QFL-54	Qianfanling	527 ± 36	11.12 ± 0.80	0.0796 ± 0.0011	986.1 ± 41.7	14.8		283,232	0.87	
HN09	Donggou	0.598	8.52	2.42 ± 0.08	296.93 ± 2.14	68		125.03		Zhu et al., 2009
HN10	Donggou	18.2	18.9	3.64 ± 0.02	346.39 ± 0.42	153		2006.75		
HN34	Sandaozhuang	1.98	11.7	1.38 ± 0.03	301.64 ± 1.12	120		306.76		
JD21	Jinduicheng	1.77	11.3	1.83 ± 0.04	295.68 ± 0.86	4		277.79		
JD23-1	Jinduicheng	5.77	17.2	3.41 ± 0.02	316.04 ± 0.47	194		640.88		
HL02-1	Shijiawan	2.20	14.4	2.09 ± 0.03	299.12 ± 2.33	79		272.96		
HL02-3	Shijiawan	3.41	17.0	1.38 ± 0.02	298.96 ± 1.20	58		362.11		
HY1-7 (1)	Yinjiagou	0.12	0.0741	1.51 ± 0.12	465.69	229.9		4367	17.8	Zhu et al., 2013
HY1-9 (1)	Yinjiagou	0.5912	0.2071	1.78 ± 0.11	567.94	170.1		9388	21.8	
HY1-9 (2)	Yinjiagou	0.1094	0.0226	1.39 ± 0.12	745.37	125.5		20,892	16.3	
HY1-9 (3)	Yinjiagou	0.8378	0.1924	1.47 ± 0.09	477.11	89.0		12,030	17.3	
HY3-7 (1)	Yinjiagou	0.0533	0.0432	5.26 ± 0.35	1095.35	595.2		7825	65.3	
HY3-7 (2)	Yinjiagou	0.5319	0.2528	5.19 ± 0.30	897.04	320.5		10,929	64.4	
HY3-10 (1)	Yinjiagou	0.2331	0.1258	0.80 ± 0.06	430.18	173.3		4616	8.9	
HY3-10 (2)	Yinjiagou	0.286	0.0979	0.84 ± 0.07	421.12	104.9		7124	9.4	
HY3-14 (1)	Yinjiagou	0.122	0.1677	2.40 ± 0.17	441.84	465.1		1861	29.1	
HY3-14 (2)	Yinjiagou	0.1616	0.096	2.28 ± 0.15	459.47	216.5		4479	27.6	

Note: $R/Ra = (^3He/^4He)_{sample}/1.4 \times 10^{-6}$; $^{40}Ar^*$ is radiogenic Ar, $^{40}Ar^* = {}^{40}Ar - (^{36}Ar \times 295.5)$; He_{mantle} is the percentage of mantle He; $^{40}Ar^*/^4He$ values of fluid inclusions in pyrite from the Yinjiagou deposit are calculated from the data from Zhu et al. (2013).

of $^3He/^4He$ produced in the crust are 0.01–0.05 Ra, $^{40}Ar/^{36}Ar \geq 45{,}000$.

He in the atmosphere is too low to exert a significant influence on He abundance and isotopic compositions of crustal fluids (Stuart et al., 1994; Ozima and Podosek, 2002). In addition, the atmospheric He contribution can be determined as the F^4He value, which is defined as the $^4He/^{36}Ar$ ratio of the sample relative to the $^4He/^{36}Ar$ ratio of atmosphere (0.1655) (Kendrick et al., 2001), such that a sample containing 100% atmospheric He will have an F^4He value of 1. The F^4He values for the pyrite samples from the Qianfanling Mo deposit are much > 1 (Table 3), indicating that the fluid contain negligible contribution of atmospheric He. Therefore, He in the ore-forming fluid of the Qianfanling Mo deposit has only two possible sources: mantle-derived He and radiogenic He produced in the crust.

The measured $^3He/^4He$ ratios in the Qianfanling Mo deposit range from 0.02438 to 0.0796 Ra (Table 3), which are similar to the characteristic values of the crust (0.01–0.05 Ra), but much lower than those of the mantle (6–9 Ra). Additionally, Tolstikhin (1978) and Kendrick et al. (2001) proposed an equation to calculate the percentage of mantle He in hydrothermal fluids on the basis of the crust-mantle dual model: He_{mantle} (%) = $(R - R_C) / (R_M - R_C) \times 100\%$, where $R_M = 8$, $R_C = 0.01$ and R represent the $^3He/^4He$ ratios of the fluids in the mantle, crust, and the sample. The calculated results of the percentage of the mantle He from the Qianfanling Mo deposit are in the range of 0.18–0.87%, with an average of 0.39% (Table 3). These values suggest that most of the He in the fluid inclusions was derived from the crust, with only a very small input from the mantle probably. This interpretation is confirmed by the ^3He versus ^4He diagram (Fig. 4).

The measured $^{40}Ar/^{36}Ar$ values of fluid inclusions hosted in the pyrite samples from the Qianfanling Mo deposit range from 694.4 to 1473.4, which is higher than the atmospheric value (295.5), indicating the involvement of atmosphere and a significantly higher concentration

Table 4
Re-Os data of molybdenite samples from the Qianfanling, Daxigou, Maogou, and Zhifang Mo deposits.

Sample	Weight (g)	Re (μg/g)		Common Os (ng/g)		^{187}Re (μg/g)		^{187}Os (ng/g)		Model age (Ma)		Data sources
		Measured	2σ	Measured	2σ	Measured	2σ	Measured	2σ	Measured	2σ	
QFL-2	0.05071	26.15	0.21	0.1412	0.0114	16.44	0.13	65.69	0.54	239.4	3.4	Y. Gao et al., 2010
QFL-3	0.05040	11.92	0.09	0.0456	0.0587	7.49	0.06	29.49	0.25	235.8	3.3	
QFL-9	0.05014	25.82	0.20	0.0341	0.0118	16.23	0.13	66.39	0.56	245.1	3.4	
QFL-9	0.05035	26.89	0.20	0.0078	0.0352	16.90	0.13	70.02	0.59	248.2	3.5	
QFL-11	0.03549	26.30	0.20	0.0486	0.0504	16.53	0.13	64.36	0.54	233.3	3.3	
QFL-13	0.05130	0.19	0.007	0.0337	0.0350	0.12	0.004	0.48	0.006	236.2	9.1	
QFL-25	0.05050	39.16	0.28	0.0342	0.0474	24.61	0.18	97.07	0.80	236.3	3.2	
DXG-1	0.02306	1.4569	0.0124	0.0645	0.0110	0.9157	0.0078	3.591	0.028	235.0	3.3	This study
DXG-5	0.03048	0.8871	0.0069	0.0323	0.0083	0.5575	0.0043	2.000	0.018	215.0	3.1	
MG-2	0.05026	4.320	0.032	0.0584	0.0358	2.715	0.020	10.46	0.09	230.9	3.3	
MG-2	0.10158	3.428	0.032	0.0270	0.0068	2.155	0.020	8.330	0.070	231.6	3.5	
MG-5	0.02588	26.159	0.191	0.0526	0.0268	16.441	0.120	65.53	0.53	238.8	3.2	
ZF-1	0.05018	28.975	0.221	0.0736	0.0331	18.211	0.139	71.43	0.61	235.0	3.3	
ZF-4	0.03006	13.341	0.102	0.0538	0.0220	8.385	0.064	32.72	0.31	233.8	3.4	
ZF-6	0.03068	17.317	0.139	0.0416	0.0320	10.884	0.087	43.20	0.36	237.7	3.4	
ZF-13	0.02025	31.590	0.239	0.0003	0.0533	19.855	0.150	78.70	0.67	237.4	3.3	
ZF-14	0.02999	12.075	0.091	0.0017	0.0386	7.590	0.057	29.78	0.27	235.0	3.3	

Note: Decay constant: λ (^{187}Re) = 1.666×10^{-11}/year (Smoliar et al., 1996). Uncertainties are absolute at 2σ with error on Re and ^{187}Os concentrations and the uncertainty in the ^{187}Re decay constant. Names of the Mo deposits: QFL = Qianfanling; DXG = Daxigou; MG = Maogou; ZF = Zhifang.

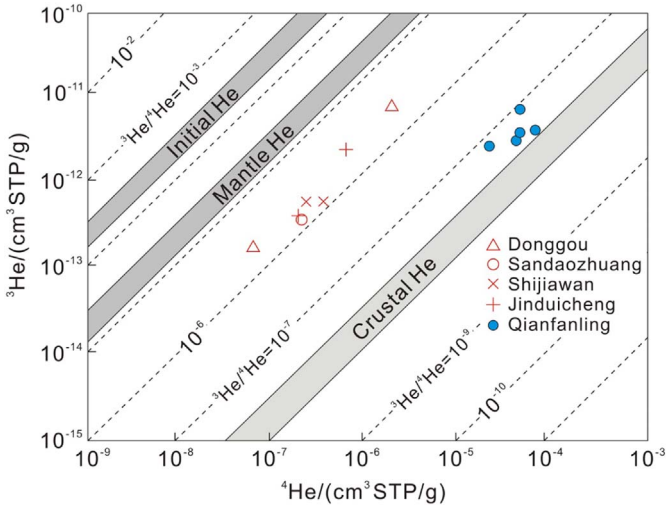

Fig. 4. Plots of ^{3}He versus ^{4}He for fluid inclusions in pyrite from the Qianfanling and four Mesozoic porphyry (-skarn) Mo deposits in the East Qinling–Dabie Mo belt. The data for the Donggou, Sandaozhuang, Jinduicheng, and Shijiawan Mo deposits are from Zhu et al. (2009).

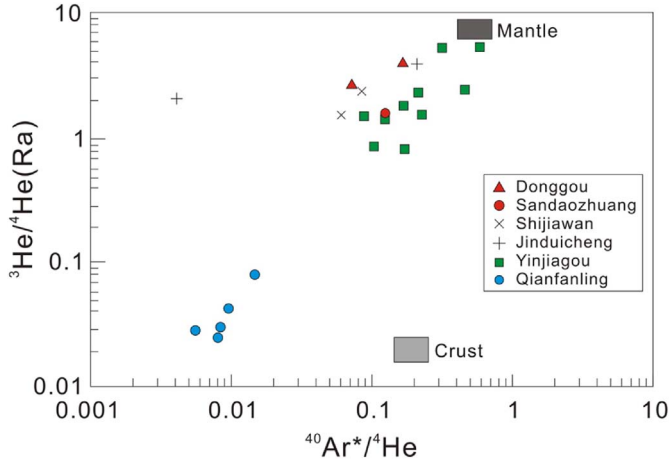

Fig. 5. ^{3}He/^{4}He versus ^{40}Ar*/^{4}He diagram of fluid inclusions in pyrite from the Qianfanling and five Mesozoic porphyry (-skarn) Mo deposits in the East Qinling–Dabie Mo belt. The fields for crust (^{3}He/^{4}He = 0.02 Ra, ^{40}Ar*/^{4}He = 0.2) and mantle (^{3}He/^{4}He = 8 Ra; ^{40}Ar*/^{4}He = 0.69 ± 0.06) are from Ballentine and Burnard (2002). The data for the Donggou, Sandaozhuang, Jinduicheng, Shijiawan, and Yinjiagou Mo deposits are from Zhu et al. (2009), and Zhu et al. (2013).

of radiogenic ^{40}Ar (^{40}Ar*) of the mantle or crustal sources (^{40}Ar/^{36}Ar values > 295.5). The very few mantle He in the fluid inclusions (0.39%), which calculated above, indicates that almost no mantle-derived fluids were involved in the ore-forming fluid. Therefore, we propose that these radiogenic ^{40}Ar were mainly derived from the crust.

Previous studies have demonstrated that geological fluids would preferentially acquire ^{4}He relative to ^{40}Ar from crustal rocks, due to the higher closure temperature of Ar (250 °C) relative to He (< 200 °C) in most minerals (Lippolt and Weigel, 1988; McDougall and Harrison, 1988; Elliot et al., 1993). Thus, we suggest that the ore-forming fluid of the Qianfanling Mo deposit have acquired not only some ^{4}He, but also a certain amount of radiogenic ^{40}Ar from crustal rocks. It also implies that the ore-forming fluid of the deposit have a relatively high temperature. This is consistent with the result of the fluid inclusion microthermometry analysis of the Qianfanling Mo deposit (Gao et al., 2013). The proportion of ^{40}Ar* can be estimated by using the measured maximum ^{40}Ar/^{36}Ar values as follows (Kendrick et al., 2001):

$$^{40}Ar^{*}(\%) = [((^{40}Ar/^{36}Ar)_{max} - 295.5)/(^{40}Ar/^{36}Ar)_{max}] \times 100$$

Estimates of the ^{40}Ar* proportion for the Qianfanling Mo deposit is 79.9%, indicating that the Ar in the ore-forming fluid was mainly derived from the mantle or crustal sources, with minor atmospheric Ar involved. Previous fluid inclusion and H–O–C isotope studies indicated that fluid-mixing was not an important process during ore deposit formation, the ore-forming fluid was mainly derived from a single deep-seated magmatic source, with little interaction of meteoric water probably (Gao et al., 2013). Therefore, we conclude that the ore-forming fluid of the Qianfanling Mo deposit was mainly derived from a deep crustal magmatic source.

On the basis of He-Ar isotope analysis of four Late Jurassic to Early Cretaceous porphyry (-skarn) type Mo deposits in the East Qinling (including Jinduicheng, Donggou, Shijiawan, and Sandaozhuang), Zhu et al. (2009) suggested that mantle-derived fluid is one of the main sources of the ore-forming fluids of these deposits (Fig. 5), with a certain amount of meteoric water involved in the ore-forming process. Additionally, using He-Ar isotopic data, Zhu et al. (2013) proposed that the formation of the Early Cretaceous Yinjiagou Mo deposit in the East Qinling is related to a mantle-derived fluid (Fig. 5). The mantle-derived fluids that were involved in the formation of these porphyry-related Mo deposits were probably related to the asthenospheric upwelling in an extensional setting (Mao et al., 2008; J.W. Mao et al., 2011). In contrast, as discussed above, the ore-forming fluid of the Qianfanling quartz-vein type Mo deposit was mainly derived from a crustal source, and both mantle and atmospheric fluids have not played an important role in the Mo mineralization.

6.2. Re contents and possible source

The Re–Os isotope system has been recognized as an effective geochemical tool not only for directly dating mineralization but also for tracing the source of ore-forming materials (e.g., Ruiz and Mathur, 1999; Mao et al., 1999). Mao et al. (1999) suggested that Re contents of molybdenite could reflect the source of the deposits, with Re contents decreasing from mantle (n × 10^{-4}) to I type (n × 10^{-5}) and to S type (n × 10^{-6}) granite-related deposits. Stein et al. (2001) proposed that deposits with a mantle component in their source have significantly higher Re contents than deposits that are derived from the crust. The Re contents in molybdenite from the Qianfanling, Daxigou, Maogou, and Zhifang quartz-vein type Mo deposits vary from 0.19 to 39.16 ppm, with an average of 17.41 ppm, indicating a crust-dominated source.

The Re contents in molybdenite from the Mesozoic Mo deposits in the East Qinling–Dabie Mo belt have been summarized in Table 5 and Fig. 6. Among these Mesozoic Mo deposits, the Triassic Huanglongpu and Huangshuian carbonatite vein type Mo (Pb) deposits, and Xigou feldspar-quartz/carbonate vein type Mo deposit contain very high Re contents in molybdenite, indicating that the ore-forming materials of these deposits were mainly derived from the mantle (Mao et al., 2008; Huang et al., 2009; Cao et al., 2014). The Majiawa and Dahu quartz-vein type Au-Mo deposits were also formed in Triassic, however, the very low Re contents in molybdenite show that these deposits were crustal source derived. The value of Re contents in molybdenite from the Qiushuwan Porphyry-skarn Cu-Mo deposit also show a deep source. Besides, the relatively high Re contents were probably associated with the high Cu/Mo ratio of the deposit (Berzina et al., 2005; Guo et al., 2006). The Re content in one molybdenite sample from the Early Cretaceous Shapoing porphyry-related Mo deposit is 282.1 ppm (Table 5), which is much higher than other porphyry-related Mo deposits in the East Qinling–Dabie Mo belt, indicating a mantle source (Su et al., 2009). Why the Shapoing Mo deposit has abnormally high Re content in molybdenite relative to other Late Mesozoic porphyry-related Mo deposits is needed to be further studied. Notably, the Mo deposits that formed after 120 Ma have relatively low Re contents in the molybdenite (Table 5; Fig. 6), suggesting that crustal materials account for a great proportion in their sources. These Mo deposits are porphyry type or

Table 5
Contents of rhenium of molybdenite and mineralization ages of the Mesozoic Mo deposits in the East Qinling–Dabie Mo belt.

Name of deposits	Type of deposits	Number of samples	Average Re (μg/g)	Age of deposits (Ma)	References
Qianfanling	Quartz-vein type Mo	6	22.35	239 ± 13	Y. Gao et al., 2010
Daxigou	Quartz-vein type Mo	2	1.172	215.0–235.0 (225.0*)	This study
Maogou	Quartz-vein type Mo	2	11.30	230.9–238.8 (233.8*)	This study
Zhifang	Quartz-vein type Mo	5	20.66	233.8–237.7 (235.8*)	This study
Majiawa	Quartz-vein type Au-Mo	5	0.6116	232 ± 11	Wang et al., 2010
Huanglongpu	Carbonatite vein type Mo (Pb)	7	283.7	221.5 ± 0.3	Stein et al., 1997
Xigou	Feldspar-quartz/carbonate vein type Mo	4	275.6	212.4 ± 2.8	Yuan et al., 2014
Huangshuian	Carbonatite vein type Mo (Pb)	8	109.1	208.4 ± 3.6	Cao et al., 2014
Dahu	Quartz-vein type Au-Mo	4	1.002	206.4 ± 3.9	Jian et al., 2015
Balipo	Porphyry Mo	5	67.67	156.3 ± 2.2	Jiao et al., 2009
Mushan	Porphyry Mo	1	109.3	155.7 ± 5.1	Li, 2009
Nantai	Porphyry-skarn Mo	6	3.474	148.8 ± 1.7	Ke et al., 2012
Qiushuwan	Porphyry-skarn Cu-Mo	6	151.8	147 ± 4	Guo et al., 2006
Nannihu-Sandaozhuang	Porphyry-skarn Mo-W	10	27.26	146.0 ± 1.1	Xiang et al., 2012
Huoshenmiao	Skarn Mo	6	70.48	145.7 ± 3.9	Wang et al., 2014
Banchang	Porphyry-skarn-vein Ag-Cu-Pb-Zn-Mo	6	47.29	145.6 ± 1.3	Mao et al., 2008
Shijiawan	Porphyry Mo	4	20.35	145.4 ± 2.1	Zhao et al., 2013
Yechangping	Porphyry-skarn Mo	6	12.05	145.3 ± 4.4	B. Mao et al., 2011
Shangfanggou	Porphyry-skarn Mo	2	19.6	144.8 ± 2.1	Li et al., 2003
Yinjiagou	Porphyry-skarn Mo-Cu-pyrite	5	40.38	143.4 ± 0.9	Wu et al., 2014
Yaochong	Porphyry Mo	6	40.29	136.9 ± 1.2	Luo et al., 2013
Shiyaogou	Porphyry Mo	5	20.26	135.2 ± 1.8	Y.L. Gao et al., 2010
Jinduicheng	Porphyry Mo	3	16.13	129–139 (133*)	Huang et al., 1994
Leimengou	Porphyry Mo	2	22.15	132.4 ± 1.9	Li et al., 2006
Yuchiling	Porphyry Mo	6	32.12	131.2 ± 1.4	Zhou et al., 2009
Qian'echong	Porphyry Mo	6	17.01	129.4 ± 1.5	Gao et al., 2014
Shapoling	Porphyry Mo	1	282.1	126.8 ± 1.7	Su et al., 2009
Bao'anzhai	Porphyry Mo	6	7.801	122.5 ± 2.7	Chen et al., 2013
Dayinjian	Porphyry-skarn Mo	4	32.64	122.4 ± 7.2	Luo et al., 2010
Tianmugou	Vein type Mo	1	13.89	121.6 ± 2.1	Yang, 2007
Zhuyuangou	Porphyry Mo	2	0.9253	120.9 ± 2.3	Huang et al., 2010
Donggou	Porphyry Mo	2	4.115	116 ± 1.7	Ye et al., 2006
Saozhoupo	Vein type Mo	4	24.64	114.3 ± 3.4	Meng et al., 2012
Donggoukou	Vein type Mo	2	6.559	114.3 ± 3.4	Meng et al., 2012
Laojieling	Vein type Mo	1	11.02	114.3 ± 3.4	Meng et al., 2012
Shapinggou	Porphyry Mo	9	4.715	113.18 ± 0.54	Huang et al., 2011
Tangjiaping	Porphyry Mo	5	7.944	113.1 ± 7.9	Yang, 2007
Nangou	Porphyry-vein type Mo	13	20.49	106.3–108.2 (107.2*)	Yang et al., 2010

Note: * is average value of model ages.

granite-associated vein type Mo deposits. Especially, the ore-forming porphyries in the Donggou, Shapinggou, and Tangjiaping Mo deposits belong to A-type granites (Gao et al., 2015), indicating that they were probably formed in an extensional setting. The mainly crustal-derived ore-forming materials have evolved during the magmatic-hydrothermal processes, leading to the formation of the Mo deposits finally. Different proportions of mantle and crustal sources in the ore-forming materials of the Mesozoic Mo deposits in the East Qinling–Dabie Mo belt were probably related to different tectonic settings and deep processes.

The Re contents in the molybdenite from the four quartz-vein type Mo deposits in this study have an average value of 17.41 ppm, which slightly higher than 10 ppm, suggesting that the ore-forming materials were mainly derived from the crustal sources, probably with less mantle components involved in the ore-forming processes. Gao et al. (2013) reported $\delta^{34}S$ values for pyrite, molybdenite and barite from the Qianfanling Mo deposit. They revealed that sulfur isotope fractionation occurred in a closed system in the Qianfanling Mo deposit and the $\delta^{34}S_{\Sigma S}$ of the ore-forming system is 2‰, indicating derivation from a deep igneous source. Therefore, we conclude that the ore-forming materials of the Qianfanling and other quartz-vein type Mo deposits were mainly derived from deep crustal igneous sources, probably with less mantle components involved.

6.3. Implications for tectonic setting and ore genesis

The Indonsinian orogeny, which occurred in South Asia, is a significant tectonic event that related to the closure of Paleo-Tethys Ocean (Fromaget, 1927; Huang, 1945; Ren, 1984). After the evolutionary processes of multi-ocean basins, multi-terrains, and multi-island arcs, several indonsinian orogenic belts were formed in Central and Southeast China as a result of the subduction and closure of the Paleo-Tethys multi-ocean basins (Ren, 1984; Xu et al., 2012). The Qinling-Dabie Orogen, which marks the boundary between the North China and Yangtze Cratons, is a key member of these indonsinian orogenic belts (G.W. Zhang et al., 2001). This orogenic belt was formed by multistage collision between the North China and Yangtze Cratons, and the final collision between the two Cratons occurred during the Triassic (e.g., Ames et al., 1993; Hacker et al., 1998; G.W. Zhang et al., 2001; Ratschbacher et al., 2003; Wu et al., 2006). During the Late Triassic, the Qinling-Dabie Orogen evolved into a post-collisional extensional domain (Mao et al., 2008; Dong et al., 2011), which is indicated by emplacement of many post-collisional intrusions, including lamprophyre dikes, rapakivi-textured granitoids, and granitic rocks with mafic microgranular enclaves (Wang et al., 2007, 2011a; Qin et al., 2010). As mentioned above, Re–Os model ages of 15 molybdenite samples from the 4 quartz-vein type Mo deposits (Qianfanling, Daxigou, Maogou, and Zhifang) range from 215.0 to 248.2 Ma, with a mean value of 235.6 Ma, which is close to the age of peak collision between the North China Craton and the Yangtze Craton. Although there is no direct temporal and spatial relationship between the formation of the quartz vein-type Mo deposits and intrusive rocks, H-O-C-S isotopic characteristics of the Qianfanling Mo deposit indicate that the ore-forming fluid and sulfur of the deposit were derived from deep igneous sources (Gao et al., 2013).

As shown in Table 1, oxidized species (CO_2 + O_2) are much more

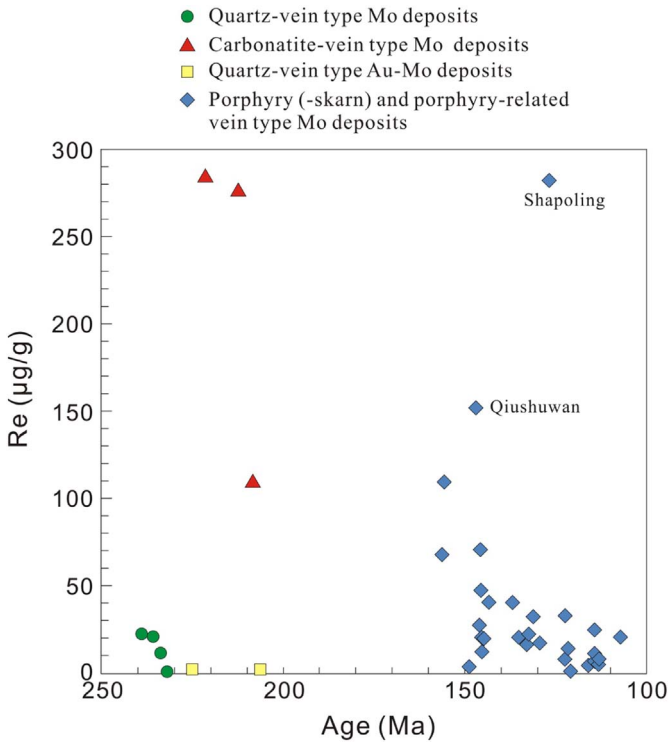

Fig. 6. Plots of total Re (ppm) in molybdenites versus age for the Mesozoic Mo deposits in the East Qinling–Dabie Mo belt. The data are from Table 5.

abundant than reduced species (CH_4 + C_2H_2 + C_2H_4 + C_2H_6 + CO) in gas compositions of fluid inclusions trapped in quartz from the Qianfanling Mo deposit, indicating that the ore-forming fluid of the deposit evolved in an oxidizing environment. Additionally, the relatively high SO_4^{2-} concentrations in liquid compositions of fluid inclusions in quartz (Table 2) also indicate that the deposit formed under conditions of high oxygen fugacity (Ohmoto, 1972; Zheng and Chen, 2000), resulting in the presence of abundant barite and barite + pyrite assemblage in the deposit. Giggenbach et al. (1994) proposed that metamorphic fluids usually have relatively high concentrations of C_2H_6, whereas there is almost no C_2H_6 in magmatic fluids. The C_2H_6 concentrations in the ore-forming fluid of the Qianfanling Mo deposit are very low (Table 1), implying that the ore-forming fluid was derived from a magmatic source. Combined with gas and liquid compositions of the ore-forming fluid, He-Ar isotopic characteristics, and Re contents in molybdenite of this study, and previous H-O-C-S isotope analysis (Gao et al., 2013), we propose that the ore-forming fluid and material of the Qianfanling Mo deposit were mainly derived from crustal magmatic sources.

During the collision between the North China and Yangtze Cratons, partial melting of deep crustal rocks under a certain condition may have caused the formation of a relatively oxidized magma. On crystallization of the oxidized magma, Mo would partition preferentially into a silicate liquid (Candela, 1992), resulting in the formation of a Mo-rich ore-forming fluid. The fluid flowed upwards through crustal fracture systems and finally formed the Qianfanling and other quartz vein-type Mo deposits.

7. Conclusion

The Mo mineralization in the quartz–vein type Mo deposits, located in the East Qinling–Dabie Mo belt, is mainly present as structurally controlled Mo-bearing quartz veins. Gas and liquid compositions of fluid inclusions in quartz from the Qianfanling quartz–vein type Mo deposit indicate that the deposit formed under conditions of high oxygen fugacity. He-Ar isotopes of fluid inclusions in pyrite indicate that the ore-forming fluid of the Qianfanling Mo deposit was mainly derived from a crustal source, and both mantle and atmospheric fluids have not played an important role in the Mo mineralization. Geochronologic data of Re–Os isotopes demonstrate that Mo mineralization in the quartz-vein type Mo deposits in the East Qinling–Dabie Mo belt took place in the Triassic (215.0–248.2 Ma), which is close to the age of peak collision between the North China and Yangtze Cratons. Re contents in molybdenite indicate that the ore-forming materials of the quartz-vein type Mo deposits were mainly derived from the crustal sources. Combined with gas and liquid compositions and He-Ar isotopes of fluid inclusions, Re contents in molybdenite, and previous studies, we conclude that the ore-forming fluid and material of the Qianfanling Mo deposit were mainly derived from crustal magmatic source.

Acknowledgements

This research was jointly supported by the Geological Survey Project (1212011220869) and the National Natural Science Foundation of China (Nos. 41272104, 41503031). We are grateful to Yang Dan, Li Chao and Ye Xianren for the assistance in the chromatography, Re–Os isotope and He-Ar isotope analyses, respectively. Meng Fang, Zhou Ke, Cheng Guoxiang and Liu Yanwei are also thanked for their help during the field investigations.

References

Ames, L., Tilton, G.R., Zhou, G.Z., 1993. Timing of collision of the Sino-Korean and Yangtse cratons: U-Pb zircon dating of coesite-bearing ecologites. Geology 21, 339–342.
Ballentine, C.J., Burnard, P.G., 2002. Production, release and transport of noble gases in the continental crust. Rev. Mineral. Geochem. 47, 481–538.
Baptiste, P.J., Fouquet, Y., 1996. Abundance and isotopic composition of helium in hydrothermal sulfides from the East Pacific Rise at 13°N. Geochim. Cosmochim. Acta 60, 87–93.
Berzina, N.A., Sotnikov, V.I., Economou-Eliopoulos, M., Eliopoulos, D.G., 2005. Distribution of rhenium in molybdenite from porphyry Cu-Mo and Mo-Cu deposits of Russia (Siberia) and Mongolia. Ore Geol. Rev. 26, 91–113.
Burnard, P.G., Hu, R.Z., Turner, G., Bi, X.W., 1999. Mantle, crustal and atmospheric noble gases in Ailaoshan gold deposits, Yunnan Province, China. Geochim. Cosmochim. Acta 63, 1595–1604.
Candela, P.A., 1992. Controls on ore metal ratios in granite-related ore systems: an experimental and computational approach. Trans. R. Soc. Edinb. Earth Sci. 83, 317–326.
Cao, J., Ye, H.S., Li, H.Y., Li, Z.Y., Zhang, X.K., He, W., Li, C., 2014. Geological characteristics and molybdenite Re-Os isotopic dating of Huangshuian carbonatite vein-type Mo (Pb) deposit in Songxian County, Henan Province. Mineral Deposits 33, 53–69 (in Chinese with English abstract).
Chen, J.F., Xie, Z., Liu, S.S., 1995. $^{40}Ar/^{39}Ar$ and fission track cooling ages of the Dabie orogenic belt. Chin. Sci. Bull. 25, 1086–1092.
Chen, W., Xu, Z.W., Lu, X.C., Yang, X.N., Li, H.C., Qu, W.J., Chen, J.Q., Wang, H., Wang, S.H., 2013. Petrogenesis of the Bao'anzhai granite and associated Mo mineralization, western Dabie orogen, east-central China: constraints from zircon U–Pb and molybdenite Re–Os dating, whole-rock geochemistry, and Sr–Nd–Pb–Hf isotopes. Int. Geol. Rev. 55, 1220–1238.
Chen, Y.J., Wang, P., Li, N., Yang, Y.F., Pirajno, F., 2017. The collision-type porphyry Mo deposits in Dabie Shan, China. Ore Geol. Rev. 81, 405–430.
Deng, X.H., Chen, Y.J., Pirajno, F., Li, N., Yao, J.M., Sun, Y.L., 2017. The geology and geochronology of the Waifangshan Mo-quartz vein cluster in eastern Qinling, China. Ore Geol. Rev. 81, 548–564.
Dong, Y.P., Zhang, G.W., Neubauer, F., et al., 2011. Tectonic evolution of the Qinling orogen, China: review and synthesis. J. Asian Earth Sci. 41, 213–237.
Du, A.D., He, H.L., Yin, N.W., Zou, X.Q., Sun, Y.L., Sun, D.Z., Chen, S.Z., Qu, W.J., 1994. A study on the Rhenium–Osmium geochronometry of molybdenites. Acta Geol. Sin. 68, 339–347 (in Chinese with English abstract).
Eide, E.A., McWilliams, M.O., Liou, J.G., 1994. $^{40}Ar/^{39}Ar$ geochronology and exhumation of high-pressure to ultrahigh-pressure metamorphic rocks in east-central China. Geology 22, 601–604.
Elliot, T., Ballentine, C.J., O'Nions, R.K., Ricchiuto, T., 1993. Carbon, helium, neon and argon isotopes in a Po basin natural gas field. Chem. Geol. 106, 429–440.
Fromaget, J., 1927. Etudes géologiques sur le nord de l'Indochine central. Bull. Fr. Serv. Géol. Indochine 16, 141–164.
Gao, X.Y., Zhao, T.P., Yuan, Z.L., Zhou, Y.Y., Gao, J.F., 2010. Geochemistry and petrogenesis of the Heyu batholith in the southern margin of the North China block. Acta Petrol. Sin. 26, 3485–3506 (in Chinese with English abstract).
Gao, Y., Li, Y.F., Guo, B.J., Cheng, G.X., Liu, Y.W., 2010. Geological characteristics and molybdenite Re-Os isotopic dating of Qianfanling quartz-vein Mo deposit in Songxian county, Western Henan Province. Acta Petrol. Sin. 26, 757–767 (in Chinese with English abstract).

Gao, Y.L., Zhang, J.M., Ye, H.S., Meng, F., Zhou, K., Gao, Y., 2010. Geological characteristics and molybdenite Re-Os isotopic dating of Shiyaogou porphyry molybdenum deposit in the East Qinling. Acta Petrol. Sin. 26, 729–739 (in Chinese with English abstract).
Gao, Y., Ye, H.S., Mao, J.W., Li, Y.F., 2013. Geology, geochemistry and genesis of the Qianfanling quartz-vein Mo deposit in Songxian County, Western Henan Province, China. Ore Geol. Rev. 55, 13–28.
Gao, Y., Mao, J.W., Ye, H.S., Li, F.L., Li, Y.F., Luo, Z.Z., Xiong, B.K., Meng, F., 2014. Geochronology, geochemistry and Sr–Nd–Pb isotopic constraints on the origin of the Qian'echong porphyry Mo deposit, Dabie orogen, east China. J. Asian Earth Sci. 85, 163–177.
Gao, Y., Mao, J.W., Ye, H.S., Meng, F., Li, Y.F., 2015. A review of the geological characteristics and geodynamic setting of the late Early Cretaceous molybdenum deposits in the East Qinling–Dabie molybdenum belt, East China. J. Asian Earth Sci. 108, 81–96.
Giggenbach, W.F., Sheppard, D.S., Robinson, B.W., et al., 1994. Grochemical structure and position of the Waiotopu geothermal field, New Zealand. Geothermaics 23, 599–644.
Guo, B.J., Mao, J.W., Li, H.M., Qu, W.J., Qiu, J.J., Ye, H.S., Li, M.W., Zhu, X.L., 2006. Re-Os dating of the molybdenite from the Qiushuwan Cu-Mo deposit in the east Qinling and its geological significance. Acta Petrol. Sin. 22, 2341–2348 (in Chinese with English abstract).
Hacker, B.R., Wang, X., Eide, E.A., 1996. The Qinling–Dabie ultra–high–pressure collisional orogen. In: Yin, A., Harriso, T.M. (Eds.), The Tectonics of Asia. Cambridge University Press, Cambridge, pp. 345–370.
Hacker, B.R., Ratschbacher, L., Webb, L., Ireland, T., Walker, D., Dong, S.W., 1998. U-Pb zircon ages constrain the architecture of the ultrahigh-pressure Qinling-Dabie orogen, China. Earth Planet. Sci. Lett. 161, 215–230.
He, Y.H., Zhao, G.C., Sun, M., Wilde, S.A., 2008. Geochemistry, isotope systematics and petrogenesis of the volcanic rocks in the Zhongtiao Mountain: an alternative interpretation for the evolution of the southern margin of the North China craton. Lithos 102, 158–178.
Hu, R.Z., Burnard, P.G., Bi, X.W., Zhou, M.F., Pen, J.T., Su, W.C., Wu, K.X., 2004. Helium and argon isotope geochemistry of alkaline intrusion-associated gold and copper deposits along the Red River-Jinshajiang fault belt, SW China. Chem. Geol. 203, 305–317.
Hu, R.Z., Burnard, P.G., Bi, X.W., Zhou, M.F., Peng, J.T., Su, W.C., Zhao, J.H., 2009. Mantle-derived gaseous components in ore-forming fluids of the Xiangshan uranium deposit, Jiangxi province, China: evidence from He, Ar and C isotopes. Chem. Geol. 266, 86–95.
Hu, R.Z., Bi, X.W., Jiang, G.H., Chen, H.W., Peng, J.T., Qi, Y.Q., Wu, L.Y., Wei, W.F., 2012. Mantle-derived noble gases in ore-forming fluids of the granite-related Yaogangxian tungsten deposit, Southeastern China. Mineral. Deposita 47, 623–632.
Huang, J.Q., 1945. The main geotectonic features in China. In: Central Geological Survey Anthology. 20. pp. 1–165 (in Chinese).
Huang, D.H., Wu, C.Y., Du, A.D., He, H.L., 1994. Re-Os isotope ages of molybdenum deposits in east Qinling and their significance. Mineral Deposits 13, 221–230 (in Chinese with English abstract).
Huang, D.H., Hou, Z.Q., Yang, Z.M., Li, Z.Q., Xu, D.X., 2009. Geological and geochemical characteristics, metallogenetic mechanism and tectonic setting of carbonatite vein-type Mo (Pb) deposits in the East Qinling molybdenum ore belt. Acta Geol. Sin. 83, 1968–1984 (in Chinese with English abstract).
Huang, F., Luo, Z.H., Lu, X.X., Chen, B.H., Yang, Z.F., 2010. Geological characteristics, metallogenic epoch and geological significance of the Zhuyuangou molybdenum deposit in Ruyang area, Henan, China. Geol. Bull. China 29, 1704–1711 (in Chinese with English abstract).
Huang, F., Wang, D.H., Lu, S.M., Chen, Y.C., Wang, B.H., Li, C., 2011. Molybdenite Re-Os isotopic age of Shapinggou Mo deposit in Anhui Province and Mesozoic Mo ore-forming stages in East Qinling-Dabie Mountain region. Mineral Deposits 30, 1039–1057 (in Chinese with English abstract).
Jian, W., Lehmann, B., Mao, J.W., Ye, H.S., Li, Z.Y., He, H.J., Zhang, J.G., Zhang, H., Feng, J.W., 2015. Mineralogy, fluid characteristics, and Re-Os age of the late Triassic Dahu Au-Mo deposit, Xiaoqinling region, Central China: evidence for a magmatic-hydrothermal origin. Econ. Geol. 110, 119–145.
Jiao, J.G., Yuan, H.C., He, K., Sun, T., Xu, G., Liu, R.P., 2009. Zircon U-Pb and molybdenite Re-Os dating for the Balipo porphyry Mo deposit in East Qinling, China, and its geological implication. Acta Geol. Sin. 83, 1159–1166 (in Chinese with English abstract).
Ke, C.H., Wang, X.X., Yang, Y., Qi, Q.J., Fan, Z.P., Gao, F., Wang, X.Y., 2012. Rock-forming and ore-forming ages of the Nantai Mo polymetallic deposit in North Qinling Mountains and its zircon Hf isotope composition. Geol. China 39, 1562–1576 (in Chinese with English abstract).
Kendrick, M.A., Burgess, R., Pattrick, R.A.D., Turner, G., 2001. Fluid inclusion noble gas and halogen evidence on the origin of Cu–porphyry mineralizing fluids. Geochim. Cosmochim. Acta 65, 2651–2668.
Kröner, A., Zhang, G., Zhou, D., Sun, Y., 1993. Granulites in the Tongbai area, Qinling belt, China: geochemistry, petrology, single zircon geochronology and implications for the tectonic evolution of eastern Asia. Tectonics 12, 245–255.
Li, M.L., 2009. Characteristics of Intermediate-acid Small Intrusive Bodies and Metallogenic System of Molybdenum-polymetallic Deposits in Mesozoic in Dabie Mountain, Henan Province (Ph. D. Dissertation). China University of Geoscience, Beijing, pp. 1–147 (in Chinese with English abstract).
Li, Y.F., Mao, J.W., Bai, F.J., Li, J.P., He, Z.J., 2003. Re-Os isotopic dating of molybdenites in the Nannihu Molybdenum (Tungsten) orefield in the Eastern Qinling and its geological significance. Geol. Rev. 49, 652–659 (in Chinese with English abstract).
Li, Y.F., Mao, J.W., Hu, H.B., Guo, B.J., Bai, F.J., 2005. Geology, distribution, types and tectonic settings of Mesozoic molybdenum deposits in East Qinling area. Mineral Deposits 24, 292–304 (in Chinese with English abstract).
Li, Y.F., Mao, J.W., Liu, D.Y., Wang, Y.T., Wang, Z.L., Wang, Y.T., Li, X.F., 2006. SHRIMP zircon U-Pb and molybdenite Re-Os datings for the Leimengou porphyry molybdenum deposit, western Henan, and its geological implications. Geol. Rev. 52, 122–130 (in Chinese with English abstract).
Li, H.M., Chen, Y.C., Ye, H.S., Wang, D.H., Guo, B.J., Li, Y.F., 2008. Mo, (W), Au, Ag, Pb, Zn minerogenetic series related to mesozoic magmatic activities in the East Qinling-Dabie Mountains. Acta Geol. Sin. 82, 1468–1477 (in Chinese with English abstract).
Li, Y., Li, N., Yang, Y.F., Wang, P., Mi, M., Zhang, J., Chen, H.J., Chen, Y.J., 2013. Geological features and geodynamic settings of the Mo deposits in the northern segment of the Dabie Mountains. Acta Petrol. Sin. 29, 95–106 (in Chinese with English abstract).
Liou, J.G., Zhang, R.Y., Wang, X.M., Eide, E.A., Ernst, W.G., Maruyama, S., 1996. Metamorphism and tectonics of high-pressure and ultrahigh-pressure belts in the Dabie-Su-Lu region, China. In: Yin, A., Harrison, T.M. (Eds.), The Tectonic Evolution of Asia. Cambridge University Press, UK, pp. 300–344.
Lippolt, H.J., Weigel, E., 1988. ^{4}He diffusion in Ar retentive minerals. Geochim. Cosmochim. Acta 52, 1449–1458.
Liu, Y.C., Jin, Y.H., Ban, Y.H., Wu, F., Fu, Z.G., Zhang, P., 2007. The distribution law of bearing ore stratum in East Qinling-Dabie mountain mineralization belt. In: China Molybdenum Industry. 31. pp. 12–17 (in Chinese with English abstract).
Lu, X.X., 1999. The Granites and the Tectonic Evolution of Qinling Orogenic Belt. Geological Publication House, Beijing (35 pp. in Chinese).
Ludwig, K.R., 2003. User's manual for Isoplot 3.00: a geochronological toolkit for Microsoft Excel. In: Berkeley Geochronology Center Special Publication, pp. 4.
Luo, M.J., Zhang, F.M., Dong, Q.Y., Xu, Y.R., Li, S.M., Li, K.H., 1991. Molybdenum Deposits in China. Henan Press of Science and Technology, Zhengzhou (452p. in Chinese).
Luo, Z.Z., Li, Y.F., Wang, Y.T., Wang, X.G., 2010. The molybdenite Re-Os age of Dayinjian molybdenum deposit in the northern margin of the Dabie Mountain, Xinxian area, Henan, China and its significance. Geol. Bull. China 29, 1349–1354 (in Chinese with English abstract).
Luo, Z.Z., Li, Y.F., Li, J.P., Wei, M.J., Li, Y., Gao, Y., 2013. The molybdenite Re-Os age of Yaochong molybdenum deposit in the north margin of the Dabie Mountain and its significance. Acta Geol. Sin. 87, 1359–1369 (in Chinese with English abstract).
Luoyang Zhongmai Mining Company, 2008. Geology Summary of Qianfanling Mo Deposit. (in Chinese).
Mao, J.W., Zhang, Z.C., Zhang, Z.H., Du, A.D., 1999. Re-Os isotopic dating of molybdenite in the Xiaoliugou W (Mo) deposit in the northern Qilian Mountain and its geological significance. Geochim. Cosmochim. Acta 63, 1815–1818.
Mao, J.W., Goldfarb, R.J., Zhang, Z.W., Xu, W.Y., Qiu, Y.M., Deng, J., 2002. Gold deposits in the Xiaoqinling-Xiong'ershan region, Qinling Mountains, central China. Mineral. Deposita 37, 306–325.
Mao, J.W., Xie, G.Q., Zhang, Z.H., Li, X.F., Wang, Y.T., Zhang, C.Q., Li, Y.F., 2005. Mesozoic large scale metallogenic pulses in North China and corresponding geodynamic settings. Acta Petrol. Sin. 21, 169–188 (in Chinese with English abstract).
Mao, J.W., Xie, G.Q., Bierlein, F., Qu, W.J., Du, A.D., Ye, H.S., Pirajno, F., Li, H.M., Guo, B.J., Li, Y.F., Yang, Z.Q., 2008. Tectonic implications from Re-Os dating of Mesozoic molybdenum deposits in the East Qinling-Dabie orogenic belt. Geochim. Cosmochim. Acta 72, 4607–4626.
Mao, J.W., Ye, H.S., Wang, R.T., Dai, J.Z., Jian, W., Xiang, J.F., Zhou, K., Meng, F., 2009. Mineral deposit model of Mesozoic porphyry Mo and vein type Pb-Zn-Ag ore deposits in the East Qinling, Central China and its implication for prospecting. Geol. Bull. China 29, 72–79 (in Chinese with English abstract).
Mao, J.W., Xie, G.Q., Pirajno, F., Ye, H.S., Wang, Y.B., Li, Y.F., Xiang, J.F., Zhao, H.J., 2010. Late Jurassic–Early Cretaceous granitoid magmatism in East Qinling, centraleastern China: SHRIMP zircon U–Pb ages and tectonic implications. Aust. J. Earth Sci. 57, 51–78.
Mao, B., Ye, H.S., Li, C., Xiao, Z.J., Yang, G.Q., 2011. Molybdenite Re-Os isochron age of Yechangping Mo deposit in western Henan Province and its geological implications. Mineral Deposits 30, 1069–1074 (in Chinese with English abstract).
Mao, J.W., Pirajno, F., Xiang, J.F., Gao, J.J., Ye, H.S., Li, Y.F., Guo, B.J., 2011. Mesozoic molybdenum deposits in the East Qinling–Dabie Orogenic belt: characteristics and tectonic settings. Ore Geol. Rev. 43, 264–293.
Markey, R., Stein, H., Morgan, J., 1998. Highly precise Re–Os dating for molybdenite using alkaline fusion and NTIMS. Talanta 45, 935–946.
McDougall, I., Harrison, T.M., 1988. Geochronology and Thermochronology by the ^{40}Ar-^{39}Ar Method. Oxford Univ. Press, Oxford, pp. 212.
Meng, F., Ye, H.S., Zhou, K., Gao, Y.L., 2012. Geological characteristics and molybdenite Re-Os isotopic dating of Mo deposits in Laojunshan area, western Henan. Mineral Deposits 31, 480–492 (in Chinese with English abstract).
Norman, D.I., Musgrave, J.A., 1994. N_2–Ar–He composition in fluid inclusion: indicators of fluid source. Geochim. Cosmochim. Acta 58, 1119–1132.
Ohmoto, H., 1972. Systematics of sulfur and carbon isotopes in hydrothermal ore deposits. Econ. Geol. 67, 551–578.
Ozima, M., Podosek, F.A., 2002. Noble Gas Geochemistry, 2nd edition. Cambridge University Press, pp. 286.
Peng, P., Zhai, M.G., Ernst, R.E., Guo, J.G., Liu, F., Hu, B., 2008. A 1.78 Ga large igneous province in the North China Craton: the Xiong'er Volcanic Province and the North China Dyke Swarm. Lithos 101, 260–280.
Pirajno, F., Ernst, R.E., Borisenko, A.S., Fedoseev, G., Naumov, E.A., 2009. Intraplate magmatism in Central Asia and China and associated metallogeny. Ore Geol. Rev. 35, 114–136.
Qin, J.F., Lai, S.C., Diwu, C.R., Ju, Y.J., Li, Y.F., 2010. Magma mixing origin for the post-collisional adakitic monzogranite of the Triassic Yangba pluton, northwestern margin

of the South China block: geochemistry, Sr-Nd isotopic, zircon U-Pb dating and Hf isotopic evidences. Contrib. Mineral. Petrol. 159, 389–409.
Ratschbacher, L., Hacker, B.R., Calvert, A., Webb, L.E., Grimmer, J.C., Mcwilliams, M.O., Ireland, T., Dong, S., Hu, J., 2003. Tectonics of the Qinling (Central China): tectonostratigraphy, geochronology, and deformation history. Tectonophysics 366, 1–53.
Ren, J.S., 1984. The Indonsinian orogeny and its significance in the tectonic evolution of China. Acta Geosci. Sin. 9, 31–44 (in Chinese with English abstract).
Ren, F.G., Li, W.M., Li, Z.H., 1996. Ore-forming Geological Conditions and Models for Gold Exploration in the Xiong'ershan-Xiaoshan Area. Geological Publishing House, Beijing (130 pp. in Chinese).
Ruiz, J., Mathur, R., 1999. Metallogenesis in continental margin: Re-Os evidence from porphyry copper deposits in Chile. In: Lambert, D., Ruiz, J. (Eds.), Applications of Radiogenic Isotopes to Ore Deposit Research and Exploration. Reviews in Economic Geology, vol. 12. pp. 59–72.
Simmons, S.F., Sawkins, F.J., Schlutter, D.J., 1987. Mantle-derived helium in two Peruvian hydrothermal ore deposits. Nature 329, 429–432.
Smith, P.E., Evensen, N.M., York, D., Szatmari, P., Oliveira, D.C., 2001. Single-crystal ^{40}Ar–^{39}Ar dating of pyrite: no fool's clock. Geology 29, 403–406.
Smoliar, M.I., Walker, R.J., Morgan, J.W., 1996. Re–Os ages of group IIA, IIIA, IVA, and IVB iron meteorites. Science 271, 1099–1102.
Stein, H.J., Markey, R.J., Morgan, M.J., Du, A.D., Sun, Y., 1997. Highly precise and accurate Re-Os ages for molybdenite from the East Qinling-Dabie molybdenum belt, Shaanxi province, China. Econ. Geol. 92, 827–835.
Stein, H.J., Markey, R.J., Morgan, J.W., Hannah, J.L., Schersten, A., 2001. The remarkable Re-Os chronometer in molybdenite: how and why it works. Terra Nova 13, 479–486.
Stuart, F.M., Turner, G., 1992. The abundance and isotopic composition of the noble gases in ancient fluids. Chem. Geol. 101, 97–109.
Stuart, F.M., Turner, G., Duckworth, R.C., Fallick, A.E., 1994. Helium isotopes as tracers of trapped hydrothermal fluids in ocean-floor sulfides. Geology 22, 823–826.
Stuart, F.M., Burnard, P.G., Taylor, R.P., Turner, G., 1995. Resolving mantle and crustal contributions to ancient hydrothermal fluids: He-Ar isotopes in fluid inclusions from Dae Hwa W-Mo mineralisation, South Korea. Geochim. Cosmochim. Acta 59, 4663–4673.
Su, J., Zhang, B.L., Sun, D.H., Cui, M.L., Qu, W.J., Du, A.D., 2009. Geological features and Re-Os isotopic dating of newly discovered Shapoling veinlet-disseminated Mo deposit in the eastern section of East Qinling Mountains and its geological significance. Acta Geol. Sin. 83, 1490–1496 (in Chinese with English abstract).
Sun, W.D., Li, S.G., Chen, Y.D., Li, Y.J., 2003. Timing of syn-orogenic granitoids in the South Qinling, Central China: constraints on the evolution of the Qinling-Dabie orogenic belt. J. Geol. 110, 457–468.
Tolstikhin, I.N., 1978. A review: some recent advances in isotope geochemistry of light rare gases. In: Alexander, E.C., Ozima, M. (Eds.), Terrestrial Rare Gases. Japan Scientific Society Press, Tokyo, pp. 27–62.
Trull, T.W., Kurz, M.D., Jenkins, W.J., 1991. Diffusion of cosmogenic ^{3}He in olivine and quartz: implications for surface exposure dating. Earth Planet. Sci. Lett. 103, 241–256.
Turner, G., Stuart, F.M., 1992. Helium/heat rations and deposition temperatures of sulfides from the ocean floor. Nature 357, 581–583.
Turner, G., Burnard, P., Ford, J.L., Gilmour, J.D., Lyon, I.C., Stuart, F.M., Gruszczynski, M., Halliday, A., 1993. Tracing fluid sources and interactions. Philos. Trans. R. Soc. Lond. A 344, 127–140.
Wang, Y.J., Fan, W.M., Guo, F., 2002. K-Ar dating of Late Mesozoic volcanism and geochemistry of volcanic gravels in the North Huaiyang belt, Dabie Orogen: constraints on the stratigraphic framework and exhumation of the northern Dabie orthogneiss complex. Chin. Sci. Bull. 47, 1668–1695.
Wang, T., Wang, X.X., Zhang, G.W., Pei, X.Z., Zhang, C.L., 2003. Remnants of a Neoproterozoic collisional orogenic belt in the core of the Phanerozoic Qinling orogenic belt (China). Gondwana Res. 26, 699–710.
Wang, X.X., Wang, T., Jahn, B.M., Hu, N.G., Chen, W., 2007. Tectonic significance of Late Triassic post-collisional lamprophyre dykes from the Qinling Mountains (China). Geol. Mag. 144, 837–848.
Wang, T., Wang, X.X., Tian, W., Zhang, C.L., Li, W.P., Li, S., 2009. North Qinling Paleozoic granite associations and their variation in space and time: implications for orogenic processes in the orogen of central China. Sci. China Ser. D Earth Sci. 52, 1359–1384.
Wang, Y.T., Ye, H.S., Ye, A.W., Li, Y.G., Shuai, Y., Zhang, C.Q., Dai, J.Z., 2010. Re-Os age of molybdenite from the Majiawa Au-Mo deposit of quartz vein type in the north margin of the Xiaoqinling gold area and its implication for metallogeny. Earth Sci. Front. 17, 140–145 (in Chinese with English abstract).
Wang, X.X., Wang, T., Castro, A., Pedreira, R., Lu, X.X., Xiao, Q.H., 2011a. Triassic granitoids of the Qinling orogen, central China: genetic relationship of enclaves and rapakivi-textured rocks. Lithos 126, 369–387.
Wang, X.X., Wang, T., Qi, Q.J., Li, S., 2011b. Temporal-spatial variations, origin and their tectonic significance of the Late Mesozoic granites in the Qinling, Central China. Acta Petrol. Sin. 27, 1573–1593 (in Chinese with English abstract).
Wang, S., Ye, H.S., Yang, Y.Q., Su, H.M., Yang, C.Y., Li, C., 2014. Molybdenite Re-Os isochron age of the Huoshenmiao Mo deposit in Luanchuan of Henan Province and its geological implications. Geol. Bull. China 33, 1430–1438 (in Chinese with English abstract).
Wu, Y.B., Zheng, Y.F., Zhao, Z.F., Cong, B., Liu, X.M., Wu, F.Y., 2006. U-Pb, Hf and O isotope evidence for two episodes of fluid-assisted zircon growth in marble-hosted eclogites from the Dabie orogen. Geochim. Cosmochim. Acta 70, 3743–3761.
Wu, G., Chen, Y.C., Li, Z.Y., Liu, J., Yang, X.S., Qiao, C.J., 2014. Geochronology and fluid inclusion study of the Yinjiagou porphyry–skarn Mo–Cu–pyrite deposit in the East Qinling orogenic belt, China. J. Asian Earth Sci. 79, 585–607.
Xiang, J.F., Mao, J.W., Pei, R.F., Ye, H.S., Wang, C.Y., Tian, Z.H., Wang, H.L., 2012. New geochronological data of granites and ores from the Nannihu-Sandaozhuang Mo (W) deposit. Geol. China 39, 458–473 (in Chinese with English abstract).
Xie, C.F., Xiong, C.Y., Hu, N., Li, J.S., 2001. A study on regional metallogenic regularity of the East Qinling-Dabie orogenic belt. Geol. Miner. Resour. South China 3, 14–22 (in Chinese with English abstract).
Xie, G.Q., Mao, J.W., Li, L.R., Ye, H.S., Wan, Y.S., Li, H.M., Gao, J.J., Zheng, R.F., 2007. SHRIMP zircon U-Pb dating for the volcanic rocks of the Dayingzi Formation in the Baofeng basin in the East Qinling and its significance. Acta Petrol. Sin. 23, 2387–2396 (in Chinese with English abstract).
Xu, Z.Q., Yang, J.S., Li, H.Q., et al., 2012. Indosinian collision-orogenic system of Chinese continent and its orogenic mechanism. Acta Petrol. Sin. 1697-1709 (in Chinese with English abstract), 28.
Yang, Z.Q., 2007. Re–Os isotopic ages of Tangjiaping molybdenum deposit in Shangcheng County, Henan and their geological significance. Mineral Deposits 26, 289–295 (in Chinese with English abstract).
Yang, D., Xu, W.Y., Cui, Y.H., Chen, W.S., Lian, Y., 2007. Determination of gaseous components in fluid inclusion samples by two-dimensional gas chromatography. In: Rock and Mineral Analysis. 26. pp. 451–454 (in Chinese with English abstract).
Yang, X.Y., Lu, X.X., Du, X.W., Li, W.M., Zhang, Z.W., Qu, W.J., 2010. Ore geochemistry, petrogenesis and metallogenic dynamics of the Nangou molybdenum district in the East Qinling orogenic belt. Acta Geol. Sin. 84, 1049–1079 (in Chinese with English abstract).
Ye, H.S., Mao, J.W., Li, Y.F., Guo, B.J., Zhang, C.Q., Liu, J., Yan, Q.R., Liu, G.Y., 2006. SHRIMP zircon U-Pb and molybdenite Re-Os dating for the superlarge Donggou porphyry Mo deposit in East Qinling, China, and its geological implication. Acta Geol. Sin. 80, 1078–1088 (in Chinese with English abstract).
Ye, X.R., Tao, M.X., Yu, C.A., Zhang, M.J., 2007. Helium and neon isotopic compositions in the ophiolites from the Yarlung Zangbo River, Southwestern China: the information from deep mantle. Sci. China Ser. D Earth Sci. 50, 801–812.
Ye, H.S., Mao, J.W., Xu, L.G., Gao, J.J., Xie, G.Q., Li, X.Q., He, C.F., 2008. SHRIMP zircon U-Pb dating and geochemistry of the Taishanmiao aluminous A-type granite in western Henan Province. Geogr. Rev. 54, 699–711 (in Chinese with English abstract).
York, D., Masliwec, A., Kuybida, P., Hanes, J.E., Hall, C.M., Kenyon, W.J., Spooner, E.T.C., Scott, S.D., 1982. $^{40}Ar/^{39}Ar$ dating of pyrite. Nature 300, 52–53.
Yuan, H.C., Wang, R.T., Jiao, J.G., Li, W.Y., Liu, W.Q., Tan, W., 2014. Re-Os isotopic ages of molybdenites from Xigou Mo deposit in Huaxian of East Qinling and their geological significanc. J. Earth Sci. Environ. 36, 120–127 (in Chinese with English abstract).
Zhang, G.W., Meng, Q.R., Yu, Z.P., Sun, Y., Zhou, D.W., Guo, A.L., 1996. Orogenic processes and dynamics of the Qinling. Sci. China Ser. D Earth Sci. 39, 225–234.
Zhang, G.W., Zhang, B.R., Yuan, X.C., Xiao, Q.H., 2001. Qinling Orogenic Belt and Continental Dynamics. Science Press, Beijing (806p. in Chinese).
Zhang, Z.W., Zhu, B.Q., Chang, X.Y., 2001. Petrogenetic-metallogenetic background and time-space relationship of the east Qinling mountain Mo ore belt, China. Geol. J. China Univ. 7, 307–315 (in Chinese with English abstract).
Zhang, C.L., Wang, T., Wang, X.X., 2008. Origin and tectonic setting of the early Mesozoic granitoids in Qinling orogenic belt. Geol. J. China Univ. 14, 304–316 (in Chinese with English abstract).
Zhao, H.J., Ye, H.S., Li, C., 2013. Re-Os dating of molybdenite from the Shijiawan molybdenum deposit in Shaanxi Province and its geological implications. Acta Petrol. Mineral. 32, 90–98 (in Chinese with English abstract).
Zheng, Y.F., Chen, J.F., 2000. Stable Isotope Geochemistry. Science Press, Beijing, pp. 1–316 (in Chinese).
Zhou, K., Ye, H.S., Mao, J.W., Qu, W.J., Zhou, S.F., Meng, F., Gao, Y.L., 2009. Geological characteristics and molybdenite Re-Os isotopic dating of Yuchiling porphyry Mo deposit in western Henan Province. Mineral Deposits 28, 170–184 (in Chinese with English abstract).
Zhu, L.M., Zhang, G.W., Guo, B., Li, B., 2009. He-Ar isotopic system of fluid inclusions in pyrite from the molybdenum deposits in south margin of North China Block and its trace to metallogenetic and geodynamic background. Chin. Sci. Bull. 54, 2479–2492.
Zhu, M.T., Zhang, L.C., Wu, G., He, H.Y., Cui, M.L., 2013. Fluid inclusions and He-Ar isotopes in pyrite from the Yinjiagou deposit in the southern margin of the North China Craton: a mantle connection for poly-metallic mineralization. Chem. Geol. 351, 1–14.